IIETA International Information and Engineering Technology Association
Advancing the World of Information and Engineering

Journal Européen des Systèmes Automatisés
Vol. 56, No. 6, December, 2023, pp. 907-916
Journal homepage: http://iieta.org/journals/jesa

Optimized PI tuning of DG-Integrated Shunt Active Power Filter Using Biogeography-Based Optimization Algorithm

Venkata Anjani Kumar G*, Damodar Reddy M

Department of Electrical and Electronics Engineering, S.V. University College of Engineering, S.V. University, Tirupathi 517502, India

Corresponding Author Email: anjishelectrical@gmail.com

https://doi.org/10.18280/jesa.560602

Received: 23 September 2023
Revised: 20 November 2023
Accepted: 4 December 2023
Available online: 28 December 2023

Keywords:
biogeography-based optimization (BBO), solar cell, particle swarm optimization (PSO), power quality, distribution generation, THD

ABSTRACT

This article proposes a biogeography-based optimization (BBO) approach to optimizing the PI controller gains of the PV integrated shunt active power filter (SAPF). This method is also used to analyze how these optimum gains affect the performance of SAPF. When nonlinear loads draw reactive power from the source, harmonics are produced, which can lead to power quality issues for the utility. Our ultimate goal is to achieve sinusoidal source current, which can only be accomplished with the help of FACT devices that enhance power quality in the distribution network. SAPF is a commonly utilized device. Solar is the most popular alternative energy source because it is the most cost-effective. Therefore, this article takes into account PV-integrated SAPF for analysis. To get the highest amount of power from a PV panel, a technique called maximum power point tracking (MPPT) is used. This technique is based on perturbation and observation (P&O) in MPPT. When the SAPF converter uses this maximum power, it also sends active power to the load, so that the SAPF converter has dual functionality like reactive power compensation (FACT) and active power supply (DG Functionality) to the load. The performance of this PV-Integrated SAPF depends on many things, like how the reference current is made, how switching pulses are made, how the voltage on the dc link is controlled, etc. In order to obtain the best possible performance from SAPF, certain design parameters, such as the gains of the PI-controller, need to be optimized. Modeling and simulation of a PV-integrated SAPF are performed in Matlab/Simulink. Gain optimization of the PI controller-based PV integrated SAPF is performed using both the proposed biogeography-based optimization method and the PSO algorithm, and the results are compared. The proposed BBO-trained PV- SAPF converter's active power injection was also investigated.

1. INTRODUCTION

Fossil fuels have been burned to meet power demand for decades, but they are nonrenewable and cannot be reused [1]. They aren't ecologically sound. Pollution-friendly and contribute to climate change, so [2] renewable energy sources like solar, wind, and geothermal are essential. There are clean sources of energy generation, such as hydro, etc., and there is an abundance of them. Photovoltaic power plants have widespread application; solar energy is naturally abundant, and electrical power is widely available. Solar power as dc from the arrays, which is converted to an alternating current one that uses an inverter. Due to the energy's reactive power balancing capabilities, this equipment can be used anywhere [3]. There are more harmonics in the network because of the rise in nonlinear electronic loads and devices. Presents of a harmonic nature as well as voltages that are powers of the fundamental frequency led to systemic cases of power degradation, and as a result, the machinery got hot. To better understand the role of alterations that happens when voltage and Currents are not proportional. The impedance of the load [4] Short-circuit current is drawn by these loads. Damage electronic devices with pulses and harmonics. Rectifiers and other electronic devices are examples of non-linear loads. Everything from computers and motors to SMPSs (switch mode power supplies) to get rid of harmonics uses passive filters, but they have a few drawbacks. Have bounds, such as in resonance, and evolve in accordance as the workload shifts. To reduce grid current harmonics, active power filters are being developed; unlike passive filters, which require an external power source, these don't affect demand levels [5, 6]. Active filters can achieve the required gain while simultaneously addressing issues with attenuation. They're diminutive, but they're more effective than passive filtering systems. Their ability to avert major active power filters can handle wider frequency ranges. Photovoltaic shunt-clearing harmonics are a common application for active filters. The module's findings or those found Maximizing power generation from PV systems while keeping costs as low as possible necessitates the use of power point tracking (MPPT) techniques [7]. Additionally, a boost converter is used to increase the voltage output. When PV is implemented, it depends on a variety of factors in the real world, including things like climate and solar radiation. There's been a lot of

study into improving old power in the grids employing various filtering strategies [8]. SAHF yields the contrasting major-minor harmonics so that it nullifies itself. Turn a nonlinear load into a linear one with linear pressure.

The goal of this work is to lessen harmonic distortion [9] in a distribution system with a non-linear load. By utilizing a shunt active power filter that is integrated with solar panels. Figure 1 represents the PV-integrated SAPF, which typically provides a current that is 90 degrees out of phase with the source current [10, 11]. As a result of the nonlinear load, the converter's output voltage dips, and the filter capacitor draws a greater amount of current than usual during the compensation process. So, in order to mitigate these unforeseen effects, it is proposed [12] that a SAPF be constructed with optimal parameters.

There has been a lot of study done on the topic of using an active power filter with a photovoltaic (PV) system. The filter's structure and tuning parameters are ignored, while a variety of methods for controlling current in a 3-phase, 4-wire distribution network are proposed in the study [13]. An improved current control approach [14] using a maximum power point tracking controller has been implemented to lessen system harmonics via a grid-connected inverter. Filtering techniques, such as a self-tuning PI controller [15, 16], have been used to decrease harmonic distortions in a grid, which comprises a voltage source converter, a hysteresis controller, and a DC voltage capacitor.

The parameters of today's automatic control systems are often optimized with the help of state-of-the-art soft computing techniques. The gains of PI controllers are optimized using particle swarm optimization (PSO) techniques [17, 18]. Evolutionary algorithm optimization techniques such as the genetic algorithm (GA) [19], bacterial foraging (BF) [20], firefly [21], ant colony optimization (ACO) [22], and differential evolution (DE) [23] have all been applied to the problem of determining the best possible gain settings for the PI controller in SAPFs.

In this study, BBO, a stochastic optimization method based on swarm intelligence, has been used for the fine tuning of PV-integrated SAPF PI parameters to control the DC link voltage to achieve the best THD. Using active power control theory, the SAPF converter also works like the DG converter.

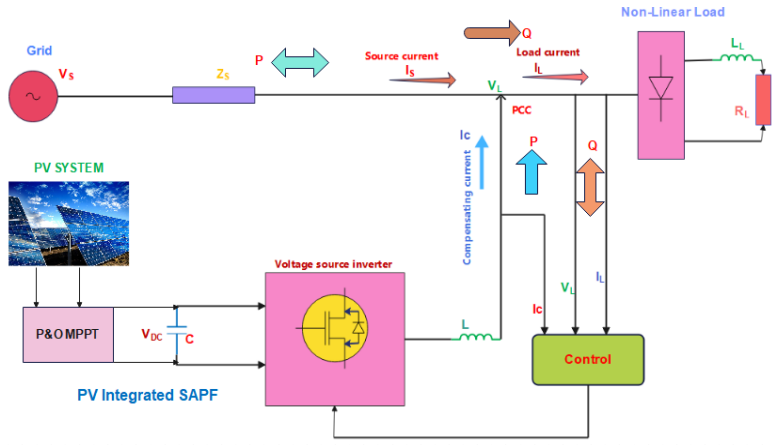

Figure 1. Model configuration of PV integrated SAPF

2. SYSTEM MODEL

The photovoltaic (PV) integrated shunt active power filter model that is the focal point of the present study is depicted in Figure 2. This model in its entirety includes the PV configuration, PV model, and PV array.

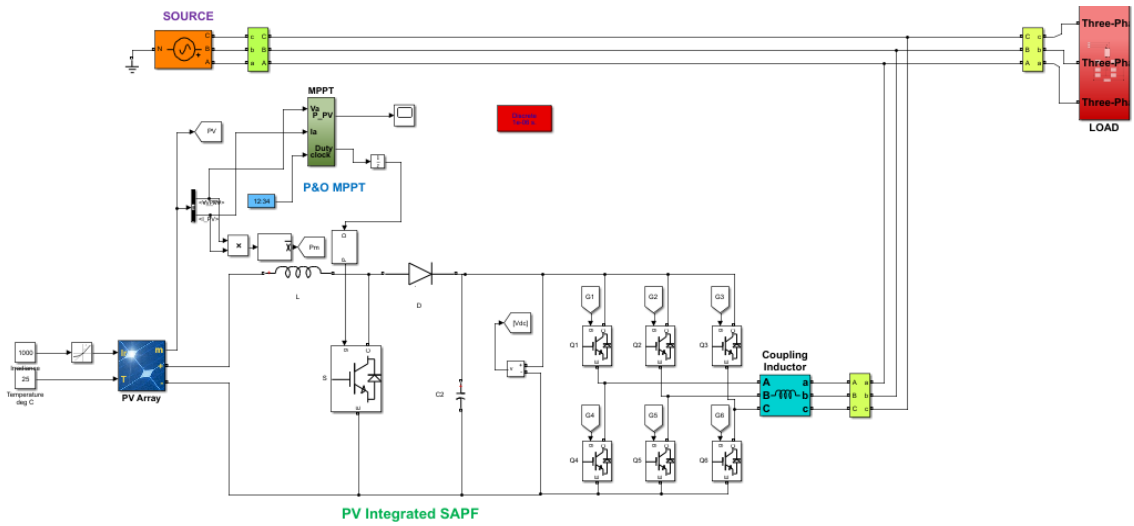

Figure 2. Simulink diagram of PV integrated SAPF when connected to non linear load

2.1 Mathematical modeling of shunt active power filters

The following assumptions need to be made in order to select the parameters for the SAPF, such as the interfacing inductance L_f and the DC capacitor C_{dc} as well as the reference dc voltage.

• The source current needs to have a sinusoidal pattern.
• The amount of distortion in the system current is no more than 5%.
• Converting takes place in a linear fashion.

The Q_C and I_h can be calculated using the two equations that are provided below.

$$Q_C=3V_CI_C = 3V_S \frac{V_C}{\omega L_f} (1 - \frac{V_S}{V_C}) \quad (1)$$

$$I_h = \frac{V_h}{m_f \omega L_f} \quad (2)$$

The V_{dcref} value can be adjusted in response to the rated voltage. The following equation is used to determine the appropriate value of C_{dc} to achieve the desired peak-to-peak voltage ripple level.

$$C_{dc} = \frac{\pi * I_c^{rated}}{\sqrt{3}\,\omega\, V_{PP}^{ripplee}} \quad (3)$$

where,

V_{dc}: The injected voltage from the filter.
L_f: The inductance of coupling for the SAPF.
C: The capacitor on the DC side of the filter.
V_s: The voltage of SAPF.
I_c: Compensating current from filter.
V_h: Harmonic voltage.

2.2 Basics of PV system

In order to convert solar energy into usable electricity, a PV system will use a series or parallel connection of PV modules or panels. Electrical output is generated via photovoltaic (PV) panels and associated mechanical and electrical connections. Solar photovoltaic (PV) output is normally dependent on solar irradiance, or the amount of sunlight available.

PV Cells, Modules, and Arrays PV cells can be connected together to make a module. Adding more modules to a PV plant works the same way, either in series or parallel, to boost the plant's power output.

A solar power plant's crucial fundamental component is PV cells. Silicon (Si) is the primary material used in solar panel construction. To generate an electric field, a thin semiconductor coating is polarized positively on one side and negatively on the other. The layer's surface is the source of the emitted electrons.

A PV cell typically produces a voltage in the range of 0.5 V to 0.7 V. As a result, the necessary output voltage and current can be obtained by connecting a series and parallel array of PV cells. In the event of partial shading, diodes in the PV array may be necessary to prevent the flow of current in the opposite direction. There is a risk of inefficiency when temperatures are very high. To counteract this, PV systems incorporate ventilation systems.

In order to convert the DC power from the PV panels into AC power for use in homes and businesses, inverter systems are installed. By connecting modules in series and parallel, higher voltage and current capacities can be achieved. The configuration is depicted in the Figure 3.

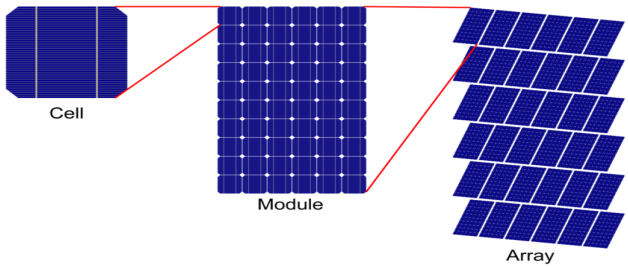

Figure 3. Interconnection diagram of solar cell, module, array

2.3 Module of PV system

The PV cell's circuit is depicted in Figure 4. It consists of only one diode, which is connected in parallel to the power supply. The function of a diode is to permit current to flow smoothly in one direction but substantially prevent it from flowing in the opposite direction. Diodes are sometimes referred to as rectifiers due to their ability to convert AC current into DC current. Both series resistance R_s and shunt resistance R_{sh} are denoted. There are two conditions for the cell, and the amount of current it draws from its source is directly related to the amount of sunlight it receives [24]. One is the potential difference between the terminals in a circuit that is open, and the other is the current in a short circuit.

When the diode is open, the voltage across it is zero, and the current through the short circuit I_{sc} is equal to the current through the current source, Voc.

The equation gives information about PV's properties.

$$I = I_L\text{-}I_0\,(e^{(v+R_s/n_s v_t Q_d)} - 1) - \frac{v+R_s}{R_{sh}}) \quad (4)$$

where, V is the array's voltage, I is the array's current, I_L is the light current, I_0 is the diode's reverse saturation current, Q_d is the diode's ideality factor, ns is the number of series cells, Rs is the series resistance, R_{sh} is the shunt resistance, V_t is the thermal voltage, and I_d is the diode current.

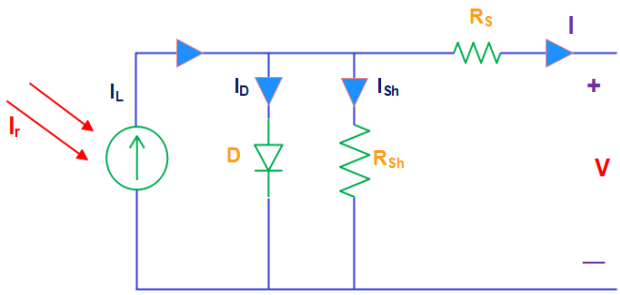

Figure 4. Single line diagram of photovoltaic system

Sun power SPR-315E-WHT-D modules were used in this study; their parameters and technical specifications are listed in Table 1.

Table 1. PV panel specifications

Parallel Strings	12
Series-connected modules per string	7
PV module name	Sun power SPR-315E-WHT-D
Max power	315.072
Open-circuit voltage (V)	64.6
Short -circuit current (A)	6.14
Voltage at MPPT (v)	54.7
Current at MPPT (a)	5.76
Irradiation (w/m^2)	1000

2.4 P&O MPPT algorithm

The P&O method uses the PV module to its full potential by maximizing efficiency in any environment. The primary benefit of this technique is the accessibility and preciseness of its algorithm, so that it can even be performed efficiently with a low-cost processor. However, a current and voltage sensor that measures the array's voltage and current is required for its implementation [25]. The power output of the PV is then calculated based on the data obtained for voltage and current.

If the duty cycle is altered by the expression P(n-1)=V(n-1)×I(n-1), and if the expression P(n)=V(n)×I(n) increases from the previous value, then n is an even number. The direction of the perturbation remains the same as P(n)=V(n)×I(n) grows larger, while when it decreases, the perturbation and, by extension, the duty cycle, switch directions [26]. Using the P&O technique, the system is represented in Figure 5.

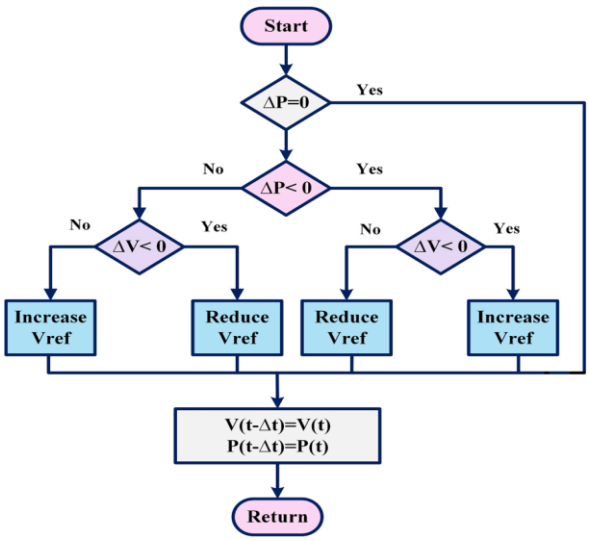

Figure 5. Flow chart representation of P&O MPPT

3. BBO OPTIMIZATION ALGORITHM

The natural phenomenon of biogeography acted as inspiration for a new metaheuristics technique called "biogeography-based optimization" (BBO). Biogeography is the study of how the geographic distribution of different species varies over time and space [27]. Simon [28] first proposed the BBO method for resolving certain continuous functions. Furthermore, this approach was developed on the basis of some principals, including species' ability to travel from island to island, the development of novel species, and the eventual extinction of extant ones. Some crucial BBO concepts are as follows:

3.1 Biogeography

According to biogeography principles, islands that are more favorable to life support systems tend to have more species, while less favorable islands tend to have fewer. Thus, the answers to the issues are like those islands. An excellent Habitat Suitability Index (HSI) value would characterize the ideal island. HSI is more commonly called "fitness" in other algorithms for population-based optimization, like the Genetic Algorithm. Suitability Index Variables (SIV) are the characteristics of the HSI. The HSI is the dependent variable in the habitat, and the SIV is taken as an independent variable.

3.2 Migration

High-HSI (or abundant species) habitats or islands will see high rates of emigration and low rates of immigration. Therefore, the higher HSI habitat is more likely to remain unchanged over time. Since these species have a high emigration rate, they are likely to relocate to nearby habitats. However, the migratory species wouldn't vanish entirely from the island of their ancestry. Those species would simultaneously appear on both islands. In most cases, the migration process would force the inferior solution to adopt the characteristics of the superior ones. If an island has a high emigration rate, it also has a low immigration rate, and vice versa. However, the island's rate of emigration is influenced by the variety of species that call it home. It stands to reason that islands with higher rates of emigration would be home to more species overall.

3.3 Mutation and elitism

In addition to migration, mutation and elitism occur during the BBO process. Mutation is a devastating ecological event. The rate at which mutations occur in various environments is known as the mutation rate. In some ecosystems, the mutation rate is proportional to the number of species present. The mutation rate in high-HSI environments is expected to be lower than in low-HSI environments. As a result, it is unusual for the mutation to preserve the good solution until the next generation is selected. Because of this mutation, novel environments would emerge to replace those with low HSI values. Without mutation, low-HSI solutions would become more prevalent, leading to a possible trap at the local optimum. Each habitat's mutation rate can be expressed as follows:

$$m_k = m_{max}\left(\frac{1 - P_k}{P_{max}}\right) \quad (5)$$

For any given habitat, the probability of having k different species is denoted by P_k, the mutation rate is denoted by m_k, and the maximum mutation rate is denoted by m_{max}, with Pmax being the maximum probability. Becauseof the mutation, a new habitat would appear in its place. The best previous solutions would also survive the elitism. All solutions, except the optimal ones with the highest probability (P_k), are equally susceptible to mutation. BBO's mutation mechanism is flexible in the same way that the mechanism of mutation that has been applied to the GA. Flow chart representation of BBO algorithm as shown in Figure 6.

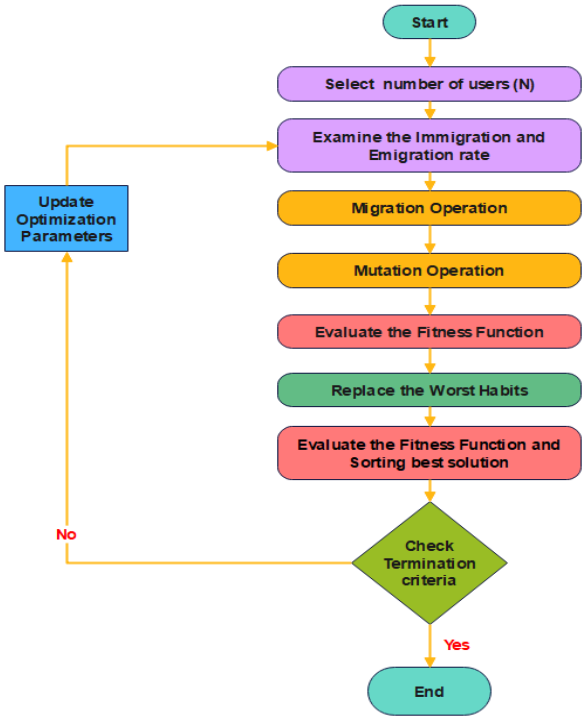

Figure 6. Flow chart representation of biogeography-based optimization (BBO)

4. PROPOSED METHODS

4.1 Tuning of PI controller by using BBO algorithm

The efficiency of a PV-integrated SAPF is dependent on the stability of the DC link voltage, which is regulated by the PI controller. Finding the gain (K_P, K_I) values of the PI controller in the critical controller is a complex mathematical process. The calculated gains are not optimal for the PI controller. To determine the best gains for the PI controller, this work implements BBO. Figure 7 shows the objective function, integral absolute error (IAE), as the discrepancy between the measured and target DC voltages. The BBO algorithm minimizes these objective functions and gives the best possible gains for the PI controller.

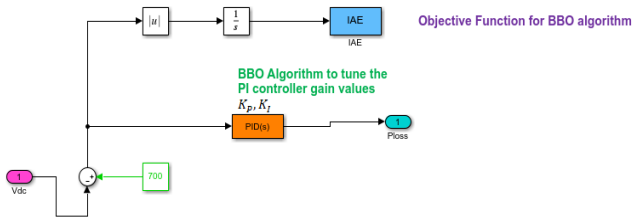

Figure 7. Simulink model of PI controller tuning with BBO algorithm

4.2 Active current coefficient control

This theory is proposed to find the actual active current required by the load, which is supplied from the PV source. Here first we need to sense the grid voltage (phase to phase) that is converted to phase to ground voltage, then these phase to ground voltages are again converted to α-β frame by using the clarck transformation, and again these α-β frame voltages are converted to an a-b-c reference frame by using the inverse clarck transformation. From that, we will get grid voltages in the a-b-c reference frame (Vg_a, Vg_b, Vg_c). These voltages pass through a band pass filter in order to remove some higher-order harmonics, and here we generate some unique vectors for synchronization of the grid with PV. And again, we need to sense the load current. With these load currents and the unique vectors, we need to find the active current coefficients for lines a, b, and c, as shown in Figure 8. Finally, we will take the average of these and get the actual active current requirement for the load (I_L).

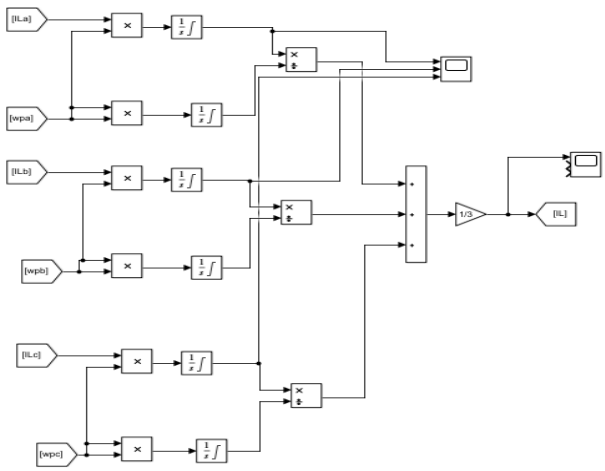

Figure 8. Simulink representation of active power coefficient theory

5. RESULTS AND DISCUSSION

This model implements a photovoltaic (PV)-based shunt active filter to mitigate undesired harmonics and enhance the power quality of the system. In order to produce gate pulses for the inverter, a hysteresis controller is built into the voltage source inverter (VSI). The model utilizes the P&O-based Maximum Power Point Tracking (MPPT) technique in order to optimize solar power extraction. The model is evaluated both with and without the inclusion of SAHF in order to analyze the network. By analyzing the data, we can determine the V-I characteristics. The shunt active filter based on photovoltaic (PV) technology is evaluated and examined using the MATLAB/SIMULINK software in order to mitigate current harmonics and facilitate power enhancement. The input supplied to the photovoltaic panel consists of solar irradiance of 1000 w/m^2 and a temperature of 25°C.Max power, open circuit voltage, and short circuit current are shown in Figure 9.

Since PV cells and other nonlinear loads are used, the source current is mostly made up of harmonic components, which affect all other loads in the distribution system. Here, the effects of a nonlinear load and the PV cell on harmonics have been looked into. A nonlinear load is used in the FFT analysis. Also, the gains of PV-SAPF's PI controller are chosen at random using trial and error. So, to improve the performance of SAPF, getting the gains of the PI controller to be as good as possible can be accomplished by employing the BBO optimization technique. In this study, the active power injection from this PV-SAPF is further examined.

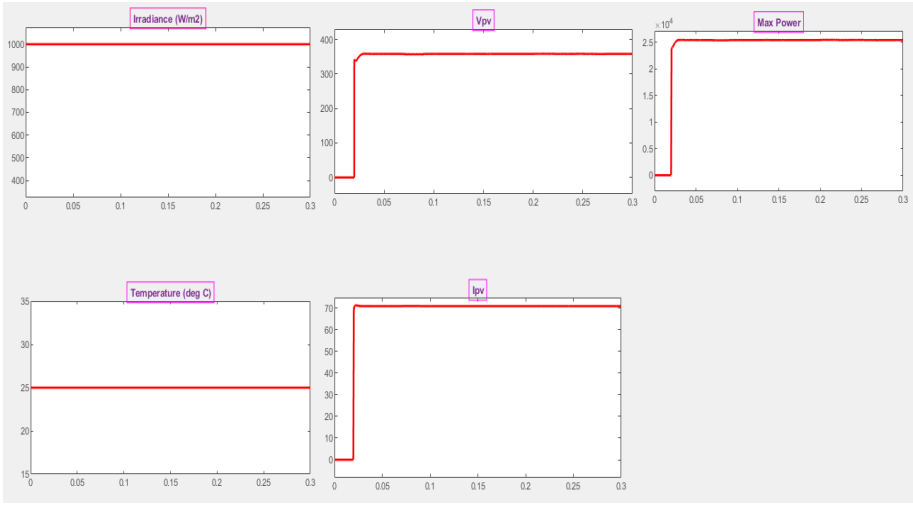

Figure 9. Output characteristics (P_{max}, V_{PV}, I_{PV}, Irradiation) of PV module

5.1 Harmonic spectrum of PV-SAPF with PSO-PI controller

Here, the PV-integrated SAPF utilizes a PSO-PI controller to control the voltage on the DC capacitor. Conventional controllers involve a lot of mathematical calculation, which is not accurate, so the gain values of the PI controller are tuned with the support of PSO's optimization algorithm. The PSO technique uses a minimization of the objective function known as the integral absolute error (IAE) to find the best possible values for the gains. With a maximum number of 100 iterations and 25 populations, For K_p and K_i, we chose 0 and 200 as the absolute minimum and maximum values, respectively.

Figure 10 shows the harmonic spectrum of PV-SAPF with the PSO-PI controller, where the THD in the grid current is 1.18%, and it shows that it is reduced from 3.08% to 1.18%.

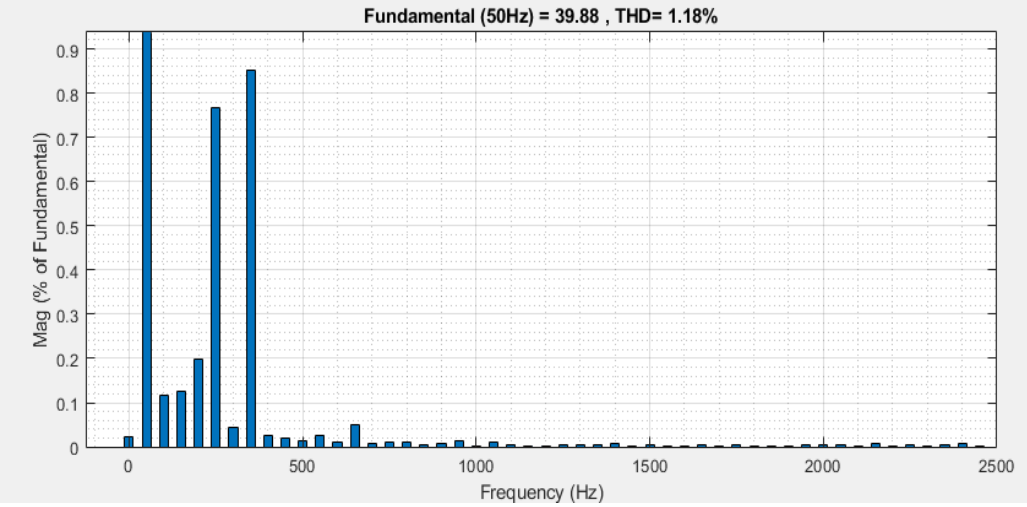

Figure 10. Grid current THD of PSO trained PI controller based PV-SAPF

5.2 Harmonic spectrum of PV-SAPF with BBO trained PI controller

Here, the PV-integrated SAPF utilizes a BBO-trained PI controller to control the voltage on the DC capacitor. A biogeography-based optimization (BBO) strategy will be used to make the necessary correction of the error voltage (IAE), which is the objective function, by adjusting the K_p and K_i gains of the PI controller. Figure 11 provides a graphic representation of source-side voltage (V_S) and source-side current (I_S) that are generated by a PV-SAPF that is controlled by a BBO-PI controller. In the event that a nonlinear load is connected to the grid at the same time, for the grid current to continue to have its normal sinusoidal shape maintained, SAPF will inject the compensating current at the PCC. Figure 12 represents the harmonic spectrum of PV-SAPF with a BBO-PI controller. From observing the figure, it is very easy to see that the THD value at the source current is 0.91%, and it shows that it is reduced from 1.18% to 0.91%. Table 2 represents the parameters of the BBO-PI controller.

Table 2. BBO configurations

BBO Parameters	Values
Maximal Iterations	100
Tuned Parameters	2
Keep Rate	0.2
Total Quantity of Reatained Habitats	5
Total Quantity of Fresh Habitats1	20
Total Populations	25
Alpha	0.9
Mutation	0.1
Emigration and Immigration Rates	1

5.2.1 Active power (P) & reactive power(Q) from PV-SAPF inverter

When PV is integrated into SAPF using active power coefficient theory, the SAPF converter will have dual functionality.

The PV-SAPF-SAPFrter works like DG; it will inject active power into the load.

The PV-SAPF-SAPFrter works like a FACT device; it will inject reactive power into the load.

Figure 13 represents the active and reactive power from the PV-SAPF inverter. From that, we can clearly observe that the PV-SAPF inverter is injecting 25.4 KW of active power and 2.054 KVAR of reactive power at the PCC.

5.2.2 Active power (P) & reactive power(Q) at load

Figure 14 represents the active power (P) and reactive power (Q) at the nonlinear load. From that, we can clearly observe that the load requires active power of 5.226 KW, which is taken from the PV-SAPF converter, and reactive power of 2.058KVAR, which is also taken from the PV-SAPF inverter.

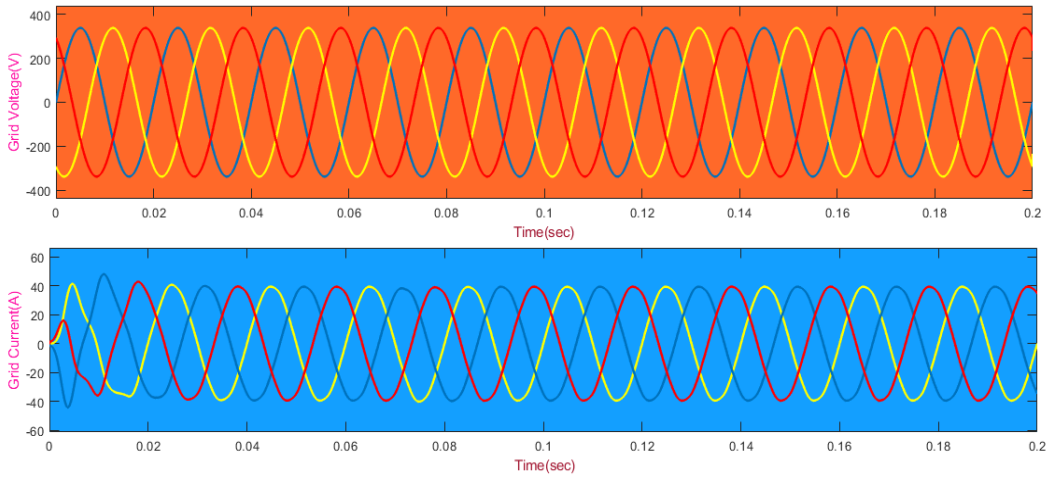

Figure 11. Source voltage and source current wave forms of BBO trained PI based PV-SAPF

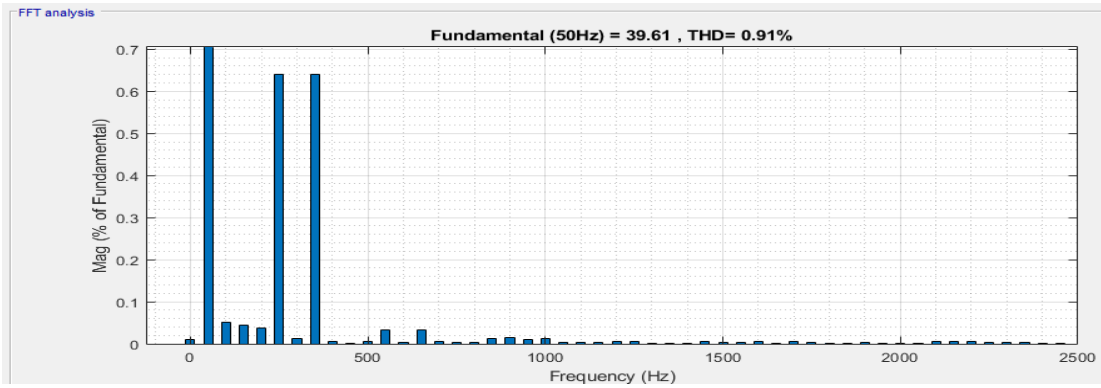

Figure 12. Grid side current THD of BBO trained PI controller based PV-SAPF

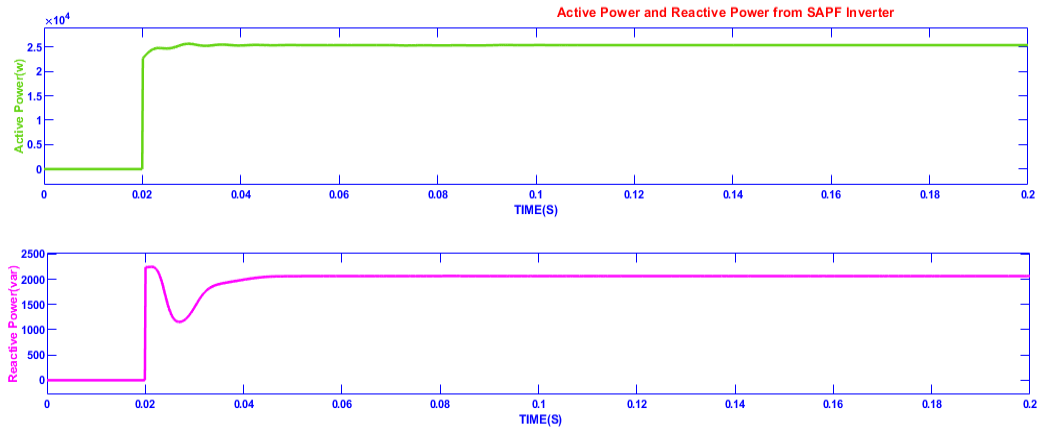

Figure 13. Active power and reactive power wave forms from PV-SAPF converter

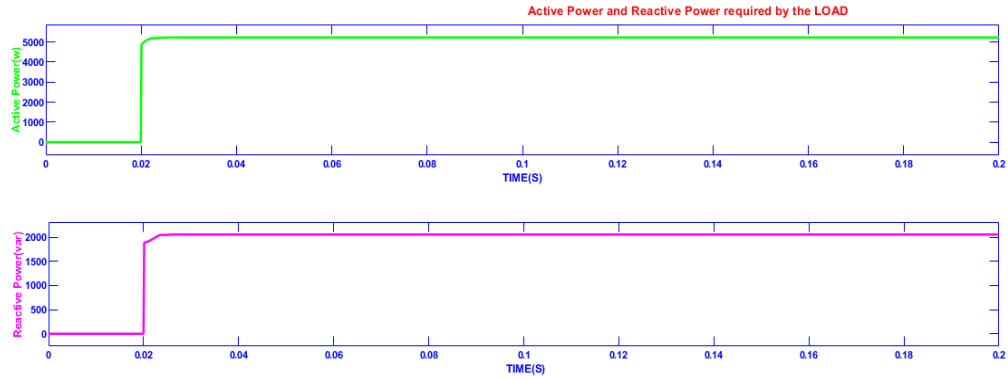

Figure 14. Active power and reactive power wave forms required by the load

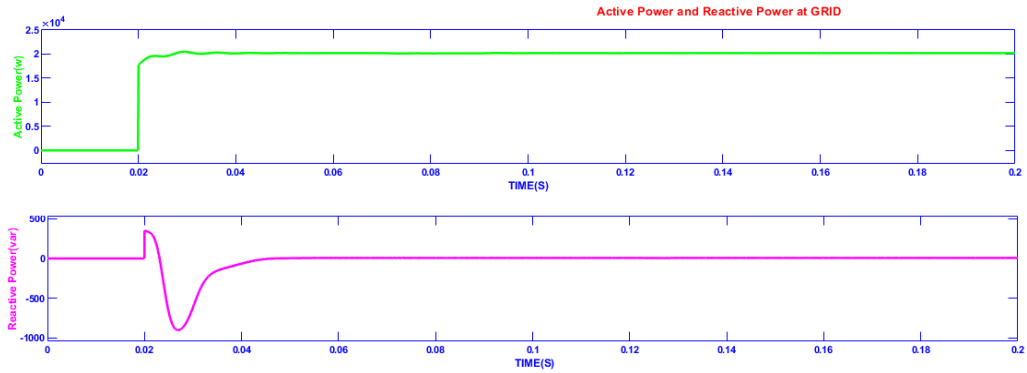

Figure 15. Active power and reactive power wave forms at GRID side

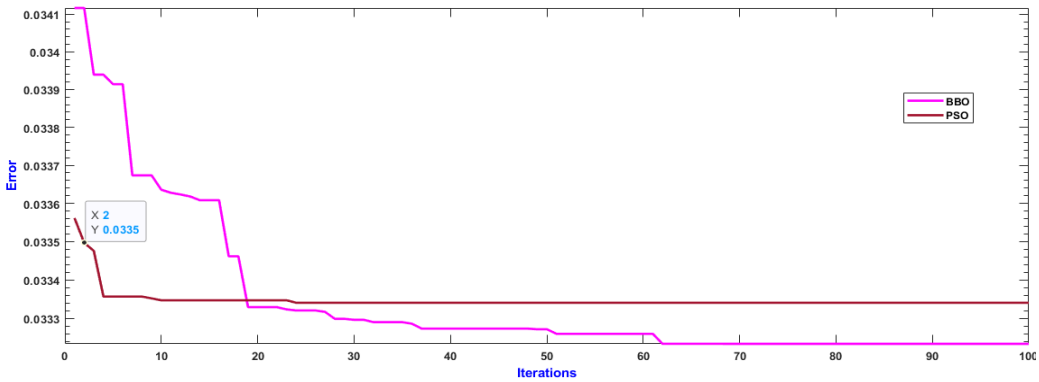

Figure 16. Converges spectrum of PSO & BBO trained PI controller based PV-SAPF

Table 3. Quantification comparisons

S_no	Type of Controller	Component	THD Value (%)
1	Without SAPF	I_S(SourceCurrent)	18.42
2	PI based PV- SAPF	I_S(SourceCurrent)	3.08
3	PV-SAPF with PSO-Trained PI cotroller	I_S(SourceCurrent)	1.18
4	PV-SAPF with BBO-Trained PI controller	I_S(SourceCurrent)	0.91

5.2.3 Active power (P) &reactive power(Q) at grid

Figure 15 represents the active power and reactive power (P&Q) at the source side; from that, we can clearly observe that the grid is not generating any reactive power (Q) for the load. At PCC PV-SAPF injecting 25.4 KW of active power, the load is taking around 5.226 KW, and the remaining 20.17 KW of active power is sent to the grid.

The converging spectrum of the BBO-PI-based PV-SAPF controller is depicted here in Figure 16, as it can be seen. It has been demonstrated that the error that is measured by the BBO-PIcontroller is less than that which is measured by the PSO-PIcontroller. The SAPF investigation findings for different incidents are listed in Table 3.

From the Table 3, we can clearly observe that the THD with a PSO-tuned PI-based PV-SAPF is 1.18%, and the proposed BBO-tuned PI-based PV-SAPF achieves a THD of 0.91%, which means the quality of grid current is better with BBO-trained PV-SAPF when compared to PSO algorithm-based PV-SAPF.

Active Power and Reactive power from SAPF inverter, Load, Grid at irradiation 0 w/m^2 and 10000 w/m^2 as given in Table 4.

Table 4. Power comparisons

Power/Irradiation	With Out DG Integration (0 W/m^2)		With DG Integration (1000 W/m^2)	
	Active Power (KW)	Reactive Power (KVAR)	Active Power (KW)	Reactive Power (KVAR)
Grid power ((P_s) & (Q_s))	5.239	0.3186	20.17	0.006
Load power ((P_L) & (Q_L))	5.226	2.058	5.226	2.058
SAPF inverte power ((P_F) & (Q_F))	0.0139	2.058	25.4	2.054

6. CONCLUSION

In this paper, we investigate the effectiveness of a PV-based shunt active filter with nonlinear loads in reducing harmonic distortion and improving overall power quality. Active filters are not the only option available, and passive filters are used for this purpose too. However, passive filters have issues such as load variation that active filters do not. It's a more cost-effective system because active filters are cheaper than passive ones. Solar irradiation and ambient temperature are two of the variables used in the PV module simulation. The P&O algorithm is used in conjunction with maximum power point tracking techniques to extract the maximum amount of power possible from PV. To increase the array's voltage, a boost converter is connected to it.

This study presents a proposed configuration for a photovoltaic (PV) integrated shunt active power filter. The configuration incorporates a biogeography-based optimization (BBO) for DC-link control, operating under ideal voltage conditions. The objective of this configuration is to improve power quality by reducing total harmonic distortion (THD). The Matlab-Simulink software runs simulations of two different scenarios and then presents the findings. The simulation results show that the THD with a PSO-tuned PI-based PV-SAPF using a PI controller is 1.18%, and the proposed BBO-tuned PI-based PV-SAPF achieves THD 0.91%, which is even better results in reducing THD in the source current than the PSO-tuned PI-based PV-SAPF. The proposed BBO-trained PV-SAPF provides not only reactive power compensation but also injects active power as required by the load.

7. FUTURE SCOPE

This suggested shunt active power filter will be implemented in hardware-in-loop in the future. The response of the PV-integrated SAPF can be improved through the implementation of an ANN, an ANFIS controller using BBO, as well as additional optimization strategies.

REFERENCES

[1] Gill, A., Singh, P., Jobanputra, J.H., Kolhe, M.L. (2022). Placement analysis of combined renewable and conventional distributed energy resources within a radial distribution network. AIMS Energy, 10(6): 1216-1229. https://doi.org/10.3934/ENERGY.2022057

[2] Mishra, A., Chauhan, S., Karuppanan, P., Suryavanshi, M. (2021). PV based shunt active harmonic filter for power quality improvement. In 2021 International Conference on Computing, Communication, and Intelligent Systems (ICCCIS), Greater Noida, India, pp. 905-910. https://doi.org/10.1109/ICCCIS51004.2021.9397214

[3] Abdellah, K., Teta, A., Rezaoui, M.M., Khadar, S. (2022). Interactive PV-shunt active power filter with fuzzy-MPPT controller for power quality improvement. In 2022 5th International Conference on Power Electronics and their Applications (ICPEA), Hail, Saudi Arabia, pp. 1-5. https://doi.org/10.1109/ICPEA51060.2022.9791143

[4] Agrawal, H., Talwariya, A., Gill, A., Singh, A., Alyami, H., Alosaimi, W., Ortega-Mansilla, A. (2022). A fuzzy-genetic-based integration of renewable energy sources and E-Vehicles. Energies, 15(9): 3300. https://doi.org/10.3390/en15093300

[5] Gill, A., Bali, H., Choudhary, A. (2022). Placement of renewable distributed energy resources in the radial distribution network to overcome the losses and air pollution. Asian Journal of Water, Environment and Pollution, 19(6): 119-125. https://doi.org/10.3934/energy.2022057

[6] Prince, S.K., Panda, K.P., Patowary, M., Panda, G. (2022). FPA tuned extended Kalman filter for power quality enhancement in PV integrated shunt active power filter. In 2019 international conference on computing, power and communication technologies (GUCON), New Delhi, India, pp. 257-262.

[7] Shiva, C., Bhavani, R., Prabha, N.R. (2017). Power quality improvement in a grid integrated solar PV system. In 2017 IEEE International Conference on Intelligent Techniques in Control, Optimization and Signal Processing (INCOS), Srivilliputtur, India, pp. 1-6. https://doi.org/10.1109/ITCOSP.2017.8303144

[8] Gill, A., Singh, P. (2021). Optimal penetration of distributed generation system in radial distribution network using adaptive scheme. In 2021 International Conference on Electrical, Electronics and Computing Technology (EECT 2021), Xiamen, China. https://doi.org/10.1088/1742-6596/1914/1/012027

[9] Wagner, V.E., Balda, J.C., Griffith, D.C., McEachern, A., Barnes, T.M., Hartmann, D.P., Phileggi, D.J., Emannuel, A.E., Horton, W.F., Reid, W.E., Ferraro, R.J., Jewell, W.T. (1993). Effects of harmonics on equipment. IEEE Transactions on Power Delivery, 8(2): 672-680. https://doi.org/10.1109/61.216874

[10] Raju, N.R., Venkata, S.S., Kagalwala, R.A., Sastry, V.V. (1995). An active power quality conditioner for reactive power and harmonics compensation. In Proceedings of PESC'95-Power Electronics Specialist Conference, Atlanta, GA, USA, pp. 209-214. https://doi.org/10.1109/PESC.1995.474814

[11] Inoue, S., Shimizu, T., Wada, K. (2007). Control methods and compensation characteristics of a series

active filter for a neutral conductor. IEEE Transactions on Industrial Electronics, 54(1): 433-440. https://doi.org/10.1109/TIE.2006.885511

[12] Da Silva, S.A.O, Sampaio, L.P., Campanhol, L.B.G. (2014). Single-phase grid-tied photovoltaic system with boost converter and active filtering. In 2014 IEEE 23rd International Symposium on Industrial Electronics (ISIE), Istanbul, Turkey, pp. 2502–2507. https://doi.org/10.1109/ISIE.2014.6865013

[13] Méndez, I., Vázquez, N., Vaquero, J., Vázquez, J., Hernández, C., López, H. (2015). Multifunctional grid-connected photovoltaic system controlled by sliding mode. In IECON 2015-41st Annual Conference of the IEEE Industrial Electronics Society, Yokohama, Japan, pp.1339-1344. https://doi.org/10.1109/IECON.2015.7392286

[14] Tareen, W.U., Mekhilef, S., Seyedmahmoudian, M., Horan, B. (2017). Active power filter (APF) for mitigation of power quality issues in grid integration of wind and photovoltaic energy conversion system. Renewable and Sustainable Energy Reviews, 70: 635-655. https://doi.org/10.1016/j.rser.2016.11.091

[15] Jayasankar, V.N., Vinatha, U. (2018). Advanced control approach for shunt active power filter interfacing windsolar hybrid renewable system to distribution grid. Journal of Electrical Systems, 4(2): 88-102.

[16] Jajarmi, H.I., Mohamed, A, Shareef, H., Subiyanto, S. (2012). A new method for calculating the reference current of shunt active power filters based on recursive discrete Fourier transform. International Review on Modelling and Simulations, 5(4), 1439-1446.

[17] Tamer, A., Zellouma, L., Benchouia, M.T., Krama, A. (2021). Adaptive linear neuron control of three-phase shunt active power filter with anti-windup PI controller optimized by particle swarm optimization. Computers & Electrical Engineering, 96: 107471. https://doi.org/10.1016/j.compeleceng.2021.107471

[18] Dubey, A.K., Dubey, S.P., Tomar, A.S. (2013). Performance analysis of PSO based hybrid active filter for harmonic and reactive power compensation under non-ideal mains. In 2013 International Conference on Advanced Electronic Systems (ICAES), Pilani, India, pp. 202−206. https://doi.org/10.1109/ICAES.2013.6659392

[19] Diab, M., El-Habrouk, M., Abdelhamid, T.H., Deghedie, S. (2019). Switched capacitor active power filter optimization using nature-inspired techniques. In 2019 21st International Middle East Power Systems Conference (MEPCON), Cairo, Egypt, pp. 556-561. https://doi.org/10.1109/MEPCON47431.2019.9008148

[20] Sharaf, A., Pandey, R., Singh, M., Jhapte, R. (2017). Elimination of harmonics using bacterial foraging optimized shunt active power filter. In 2017 Recent Developments in Control, Automation & Power Engineering (RDCAPE), Noida, India, pp. 354-359. https://doi.org/10.1109/RDCAPE.2017.8358296

[21] Gowtham, N., Shankar, S., Rao, K.U. (2017). Enhanced firefly algorithm for PQ improvement of wind energy conversion system with UPQC. In TENCON 2017-2017 IEEE Region 10 Conference,Penang, Malaysia, pp. 757-762. https://doi.org/10.1109/TENCON.2017.8227961

[22] Vishwakarma, A.P., Singh, K.M. (2020). Comparative analysis of adaptive PI controller for current harmonic mitigation. In 2020 International Conference on Computational Performance Evaluation (ComPE), Shillong, India, pp. 643-648. https://doi.org/10.1109/ComPE49325.2020.9200057

[23] Biswas, P.P., Suganthan, P.N., Amaratunga, G.A.J. (2017). Minimizing harmonic distortion in power system with optimal design of hybrid active power filter using differential evolution. Applied Soft Computing, 61: 486−496. https://doi.org/10.1016/j.asoc.2017.08.031

[24] Noui, S., Tabbache, B., Berkouk, E.M., Benbouzid, M. (2022). A pulse-width modulation control approach for the high-voltage gain operation of a z-source neutral-point clamped inverters. IETE Journal of Research, 1-20. https://doi.org/10.1080/03772063.2021.2021813

[25] Celikel, R., Yilmaz, M., Gundogdu, A. (2022). A voltage scanning based MPPT method for PV power systems under complex partial Shading conditions. Renewable Energy, 184: 361-373. https://doi.org/10.1016/j.renene.2021.11.098

[26] Pal, R.S., Mukherjee, V. (2021). A novel population based maximum point tracking algorithm to overcome partial shading issues in solar photovoltaic technology. Energy Conversion and Management, 244: 114470. https://doi.org/10.1016/j.enconman.2021.114470

[27] Huggett, J.R. (2004). Fundamentals of Biogeography. Rouledge, London.

[28] Simon, D. (2008). Biogeography-based optimization. IEEE Transactions on Evolutionary Computation, 12(6): 702-713. https://doi.org/10.1109/TEVC.2008.919004